

# Atom probe analysis of planar multilayer structures

D. J. Larson<sup>a)</sup>

*Recording Head Operations, Seagate Technology, 7801 Computer Avenue South, Minneapolis, Minnesota 55435*

R. L. Martens and T. F. Kelly

*Department of Materials Science and Engineering, University of Wisconsin, Madison, Wisconsin 53706*

M. K. Miller

*Metals and Ceramics Division, Oak Ridge National Laboratory, P.O. Box 2008, Oak Ridge, Tennessee 37831*

N. Tabat

*Recording Head Operations, Seagate Technology, 7801 Computer Avenue South, Minneapolis, Minnesota 55435*

Atom probe field ion microscopy has been used to analyze a planar-deposited layered structure in plan view. The specimens were prepared with a newly developed method that involves a combination of photolithography and focused ion-beam milling. A multilayer structure consisting of {Ta/CoFe/(Cu/CoFe)<sub>15</sub>/Ru/(CoFe/Ru)<sub>5</sub>/Ru/NiFe} was sputter deposited for use as a test stack. The corresponding thicknesses of these layers were 7/13(3/3)/50/(3/1)/50/150 nm. The nanometer-scale periodicity of the Cu/CoFe stack is readily apparent in transmission electron microscopy images of a field ion specimen fabricated from this material, suggesting that the specimen preparation procedure does not lead to destruction of the multilayer structure. Atom probe analysis of the bulk NiFe layer and the Ru/NiFe interface revealed the distribution of impurity atoms in the film, and these may affect the magnetic properties of the multilayers. Whereas a uniform distribution of C, N and Ar was observed, segregation of O was observed in the NiFe layer within  $\sim 0.25$  nm of the interphase interface, with a concentration greater than 20 times that found in the bulk of the NiFe layer. © 2000 American Institute of Physics. [S0021-8979(00)17308-6]

## INTRODUCTION

Artificial multilayer film (MLF) structures are an integral part of advanced magnetic sensors such as spin valve magnetoresistive elements.<sup>1</sup> The interfaces between the individual layers in spin valves influence the magnitude of the giant magnetoresistive effect. Structural characterization with high spatial resolution, especially at layer interfaces, can assist in the optimization of device performance with respect to processing and operating conditions. There is a crucial need for characterization techniques that can accurately map the composition of these layers, and their interfaces, at the near-atomic scale.

Atom probe field ion microscopy (APFIM)<sup>2</sup> is one technique that has the capability to characterize the local structure and composition of multilayer film devices with sufficiently high spatial resolution. However, specimen preparation for APFIM of MLF materials is challenging, since a suitable specimen essentially consists of a sharply pointed needle (tip radius  $< 50$  nm) containing the layers of interest on the end of the needle. Previously, atom probe field ion microscopy research has been limited to layers which have been sputtered onto a previously evaporated field ion specimen<sup>3-5</sup> or planar-deposited structures with layers oriented parallel to the direction of the analysis.<sup>6,7</sup> The present work reports atom probe analyses of planar-deposited multilayer structures from specimens fabricated with the layers in plan view at the apex of the specimen.

## EXPERIMENT

Field ion microscopy was performed in  $\sim 1 \times 10^{-3}$  Pa of Ne. Three-dimensional atom probe analysis was performed in an energy-compensated optical position-sensitive atom probe at a pressure of  $\sim 5 \times 10^{-9}$  Pa with a pulse fraction of 20% and a pulse repetition rate of 1500 Hz. The specimen temperature was  $\sim 60$  K for both the field ion microscopy and atom probe analyses. All compositions are given in atomic percent and all error bar measurements are given as  $1\sigma$ .

A multilayer structure consisting of {Ta/CoFe/(Cu/CoFe) $\times 15$ /Ru(CoFe/Ru) $\times 5$ /Ru/NiFe} having layer thicknesses of 7/13(3/3)/50(3/1)/50/150 nm was deposited using a dc magnetron sputtering system (base pressure  $\sim 5 \times 10^{-6}$  Pa) onto low resistivity ( $\rho \sim 0.05 \Omega \text{ cm}$ ) silicon (100) substrates. The low resistivity substrate allowed the samples to transmit the high voltage pulses required for atom probe analysis.<sup>8</sup> Films were typically deposited in 2–5 mTorr ( $2.7\text{--}6.7 \times 10^{-1}$  Pa) of Ar at a rate of 0.1–0.2 nm/s. Small variations in these conditions were used to ensure optimum deposition conditions in each layer.

Prior to deposition, the substrate was lithographically patterned and partially etched into high aspect ratio posts  $\sim 4 \mu\text{m} \times \sim 4 \mu\text{m} \times \sim 100 \mu\text{m}$  tall. Following deposition, the posts were removed from the wafer by fracturing them near the base and then attaching them (with Ag-based epoxy) to metallic needles to facilitate further handling. This specimen fabrication process has several advantages compared to previous methods<sup>3-7</sup> including the fact that (1) the layers are deposited onto a planar substrate, (2) numerous specimens

<sup>a)</sup>Electronic mail: david\_j\_larson@notes.seagate.com

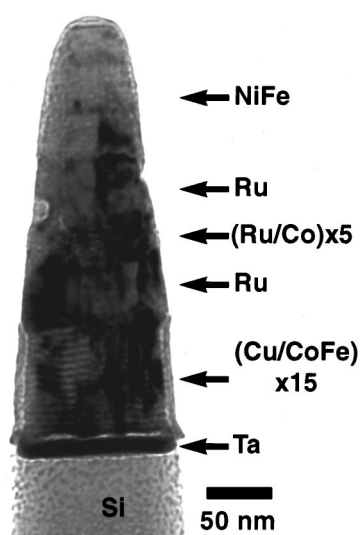


FIG. 1. Field ion specimen which contains a portion of the 380 nm multilayer film structure prepared by focused ion-beam milling.

can be fabricated simultaneously, and (3) specimens can be easily annealed directly on the wafer.

## RESULTS

The specimens were sharpened with annular focused ion-beam milling<sup>9,10</sup> into the needle geometry<sup>2</sup> required for atom probe analysis, as shown in Fig. 1. A thick (380 nm) test stack structure was fabricated in order to ensure that a portion of the stack would remain unmilled on the apex of the specimen after focused ion-beam milling.

The feasibility of fabricating the desired specimen geometry is demonstrated by Fig. 1, which shows a sharp ( $\sim 30$  nm radius) field-ion specimen in an orientation normal to a planar surface and sharpened such that the apex is formed from a region within  $\sim 50$  nm of that surface. The clearly apparent Cu/CoFe layered structure near the base of the stack in Fig. 1 suggests that deposition onto a small flat surface ( $\sim 10 \mu\text{m}^2$ ) does not adversely affect layer quality.

A field ion image of the fine-grained NiFe layer is shown in plan view, Fig. 2. This layer is positioned at the specimen apex in Fig. 1. Atom probe analysis may be performed at any point in this image, as shown in Fig. 2. The average composition of the NiFe layer shown in Fig. 2, from all of the measurements denoted in Fig. 2, was  $82.3 \pm 0.5\%$  Ni- $17.45 \pm 0.5\%$  Fe- $0.16 \pm 0.06\%$  C- $0.09 \pm 0.04\%$  O (with no significant Ga detected). This compares well with the nominal target composition of 82.6% Ni-17.4% Fe and with x-ray photoelectron spectroscopy measurements of 82.5% Ni-17.5% Fe.

The interface between the NiFe cap layer and the underlying Ru layer was analyzed by atom probe analysis, as shown in Fig. 3(a) (the orientation is reversed from that in Fig. 1). The Ru atoms are denoted by large, dark spheres, the Ni atoms by small, light spheres and the Fe atoms by small, dark spheres. A projection of a reconstructed volume with dimensions  $12 \times 12 \times 4$  nm shows the spatial distribution of the impurity elements O (light) and C (dark) [Fig. 3(b)] and N (light) and Ar (dark) [Fig. 3(c)]. A larger extent of the Ru

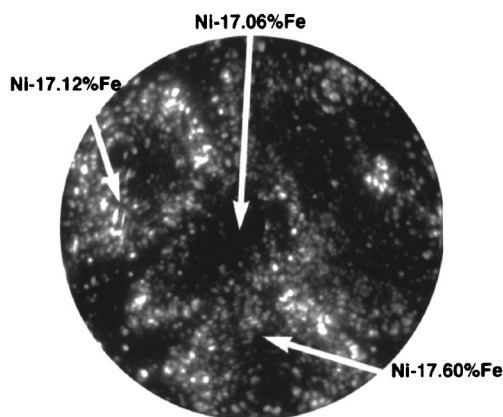


FIG. 2. Field ion micrograph of the apex region of a specimen similar to the one shown in Fig. 1 which shows a portion of the NiFe layer. Compositional analyses were obtained at the three points indicated.

layer is not contained in this reconstruction due to sample fracturing during the analysis. At a distance greater than  $\sim 2$  nm from the NiFe/Ru interface, the average composition of the NiFe layer was  $81.7 \pm 0.5\%$  Ni- $17.5 \pm 0.5\%$  Fe- $0.14 \pm 0.05\%$  Ru- $0.13 \pm 0.04\%$  O- $0.11 \pm 0.04\%$  C- $0.09 \pm 0.04\%$  Ga- $0.11 \pm 0.04\%$  Ar- $0.05 \pm 0.03\%$  N. These atom probe data provide quantification of the concentration of impurity elements, including Ar, incorporated into the films during the deposition (and subsequent processing steps) and include the position of these impurities with respect to the interfaces. The concentration of the various elements corresponding to the reconstruction in Fig. 3 may be quantified in a compositional profile with the abscissa approximately normal to the interface plane, as shown in Fig. 4.

The apparent width of the NiFe/Ru interface (10%–90%) is  $\sim 0.5$  nm at the position of this composition profile. However, significant Ru is detected to a depth of  $\sim 1$  nm in the NiFe layer, as shown in Fig. 4.

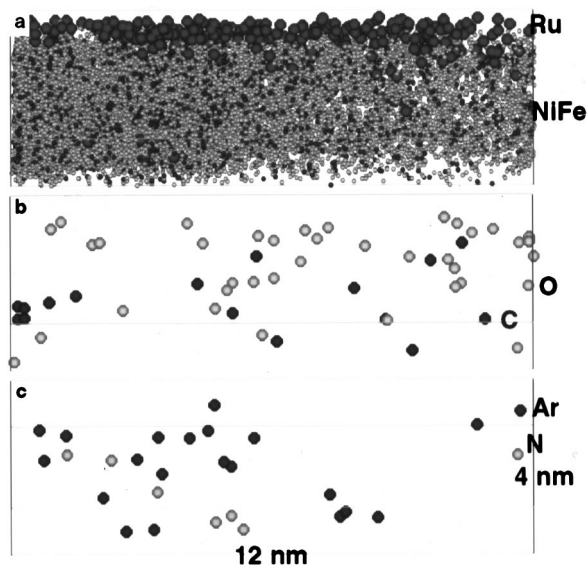


FIG. 3. Three-dimensional atom probe analysis of an interface between NiFe and Ru layers showing the distribution of (a) Ni, Fe and Ru atoms, (b) C and O atoms and (c) N and Ar atoms.

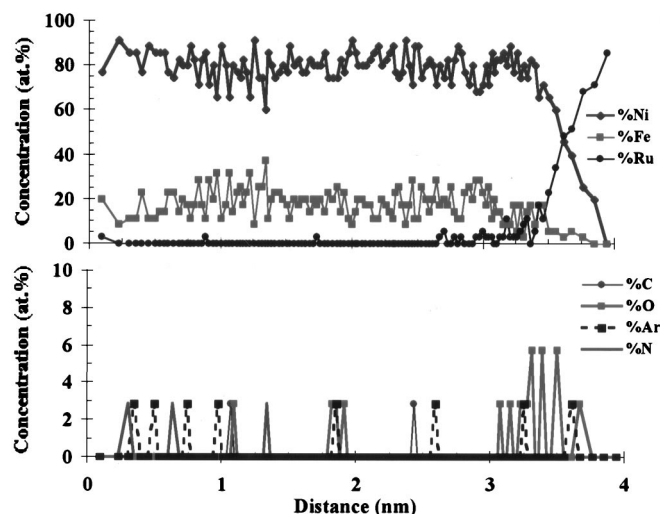


FIG. 4. Compositional profile of impurity elements across the NiFe/Ru interface shown in Fig. 3. The profile shows a small Ru presence in the NiFe near the interface and O segregation at the interface.

It is known that field ion specimens fabricated by focused ion-beam methods can suffer from the effects of implanted Ga ions.<sup>9</sup> The Ga concentration in the specimens referred to in Figs. 2–4 was less than 0.1% Ga. However, several other atom probe samples contained up to  $\sim 10\%$  Ga (near the apex region), which suggests excessive imaging with the focused ion beam during sample fabrication. Previous work has shown that layered structures can be totally destroyed by heavy focused ion-beam imaging, but at levels of  $\sim 1\%$  Ga or less, the layers are typically visible in both field ion images and atom probe analysis.<sup>6,10</sup> Clearly, care must be taken to ensure that heavy Ga implantation does not significantly modify the multilayer structure.

Gas incorporation into a growing film structure varies with parameters such as gas pressure.<sup>11</sup> Atom probe analysis can provide concentrations of gas atoms incorporated into thin films as well as the spatial distribution of these gas atoms. The data shown in Figs. 3 and 4 indicate that a minimal amount of Ar ( $\sim 0.1\%$  Ar) has been incorporated into the NiFe film and into the NiFe/Ru interface and that the Ar distribution exhibits no interfacial segregation.

The distribution of impurities that are incorporated into thin films during deposition may also influence film microstructures. A relatively uniform distribution of C and N impurities is indicated in Figs. 3 and 4; however O has segregated to the NiFe edge of the interface. There is interest in the interfacial concentrations of O in giant magnetoresistance structures because O has been proposed for use as a surfactant in these structures.<sup>12</sup> The concentration of O measured over a  $\sim 0.25$  nm region positioned on the NiFe edge of the NiFe/Ru interface is  $\sim 2.9 \pm 1.2\%$  O, which is more than a factor of 20 greater than that measured in the bulk.

The enhanced O concentration at the NiFe/Ru interface may arise due to adsorption during the brief pause in the

deposition process while sputtering targets were switched. Oxygen is more reactive than the other detected impurities and the exposed Ru surface may have oxidized during the switch to NiFe deposition conditions. There is also a possibility, but very unlikely for Ar, that defects and impurities were incorporated into the samples during focused ion-beam milling.

This work demonstrates that atom probe analyses may be obtained from planar-deposited multilayers in a direction normal to the stack and demonstrates the feasibility of this characterization technique for these nanoscale multilayer structures. Future work includes refinement of the specimen preparation technique to enable accurate positioning of stack regions for atom probe analysis and employment of a dual-beam focused ion-beam instrument in order to minimize Ga implantation and damage.

## ACKNOWLEDGMENTS

The authors would like to thank Dr. I. M. Anderson, Dr. N. D. Evans, and Dr. R. P. Michel for helpful comments and R. J. Viellieux, Dr. R. L. Hipwell, and Dr. B. D. Wismann for their contributions to this research. This research was sponsored, in part, by the Division of Materials Sciences, US Department of Energy and by a cooperative research and development agreement with the Honeywell Solid State Electronics Center and Nonvolatile Electronics Inc. sponsored by the Laboratory Technology Research Program, US DOE, both under Contract No. DE-AC05-96OR22464 with Lockheed Martin Energy Research Corp., and by the SHaRE Program under Contract No. DE-AC05-76-OR00033 with Oak Ridge Associated Universities. This research was conducted, in part, utilizing the Shared Research Equipment User Program facilities at Oak Ridge National Laboratory.

<sup>1</sup>S. S. P. Parkin, *Annu. Rev. Mater. Sci.* **25**, 357 (1995).

<sup>2</sup>M. K. Miller, A. Cerezo, M. G. Hetherington, and G. D. W. Smith, *Atom Probe Field Ion Microscopy* (Oxford University Press, Oxford, 1996).

<sup>3</sup>A. K. Petford-Long, A. Cerezo, and J. M. Hyde, *Ultramicroscopy* **47**, 367 (1992).

<sup>4</sup>A. K. Petford-Long, R. C. Doole, A. Cerezo, J. S. Conyers, and J. P. Jakubovics, *J. Magn. Magn. Mater.* **126**, 117 (1993).

<sup>5</sup>T. Al-Kassab, M.-P. Macht, V. Naundorf, H. Wollenberger, S. Chambrelan, F. Danoix, and D. Balvette, *Appl. Surf. Sci.* **94/95**, 306 (1995).

<sup>6</sup>D. J. Larson, A. K. Petford-Long, D. T. Foord, A. Cerezo, T. C. Anthony, and G. D. W. Smith, *Appl. Phys. Lett.* **73**, 1125 (1998).

<sup>7</sup>D. J. Larson, A. K. Petford-Long, A. Cerezo, and G. D. W. Smith, *Acta Mater.* **47**, 4019 (1999).

<sup>8</sup>S. J. Sijbrandij, D. J. Larson, and M. K. Miller, *Microsc. Microanal.* **4**, 90 (1998).

<sup>9</sup>D. J. Larson, D. T. Foord, A. K. Petford-Long, T. C. Anthony, I. M. Rozdilsky, A. Cerezo, and G. D. W. Smith, *Ultramicroscopy* **75**, 147 (1998).

<sup>10</sup>D. J. Larson, D. T. Foord, A. K. Petford-Long, H. Liew, M. G. Blamire, A. Cerezo, and G. D. W. Smith, *Ultramicroscopy* **79**, 287 (1999).

<sup>11</sup>W. W. Y. Lee and D. W. Oblas, *J. Appl. Phys.* **46**, 1728 (1975).

<sup>12</sup>W. F. Egelhoff, Jr., P. J. Chen, C. J. Powell, M. D. Stiles, R. D. McMichael, J. H. Judy, K. Takano, and A. E. Berkowitz, *J. Appl. Phys.* **82**, 6142 (1998).